

## On the Integrability of the Toda Lattice

Joseph FORD, Spotswood D. STODDARD and Jack S. Turner\*

*School of Physics, Georgia Institute of Technology  
Atlanta, Georgia 30332*

*\*Center for Statistical Mechanics and Thermodynamics  
University of Texas, Austin, Texas 78712*

(Received May 7, 1973)

This paper presents a variety of computer generated evidence indicating that the Toda lattice behaves remarkably like an integrable, nonlinear system, where here integrability means that the system Hamiltonian can be brought to an obviously integrable form. In particular, we investigate Toda lattices having three and six particles, using periodic boundary conditions. While computer calculations cannot rigorously prove integrability, the evidence presented here is sufficiently strong to provide incentive for seeking the general, closed form, analytic solution or, at least, some approximation to it.

### § 1. Introduction

The Toda lattice<sup>1)</sup> is of considerable interest to physical scientists because it serves as an example of a nonlinear lattice system which may rigorously be shown to propagate certain wave forms without change of shape. Moreover the propagation of such unchanging wave forms has been observed experimentally<sup>2)</sup> in various physical systems. Additionally in the continuum limit, the Toda lattice can be shown to be described by the nonlinear Korteweg-deVries (KdV) equation,<sup>3)</sup> thereby connecting the theory<sup>1)</sup> of the Toda lattice with the KdV soliton theory<sup>3)</sup> developed by Kruskal, Zabusky, and others.

For the KdV equation the unchanging wave form, called a soliton, has been shown<sup>3)</sup> both theoretically and empirically (on a computer) to be remarkably stable. Indeed, a recent paper by Zakharov and Faddeev<sup>4)</sup> definitively establishes the validity and the source of this stability. In particular these authors prove that the KdV equation is a completely integrable Hamiltonian system, where integrability<sup>5)</sup> here means that the system Hamiltonian can be reduced to an obviously integrable (or solvable) form<sup>6)</sup> by a canonical transformation analytic in the position and momentum variables. Because of the intimate connection<sup>7)</sup> between the Toda lattice and the KdV equation, the Zakharov-Faddeev result suggests that the Toda lattice may also be integrable and its associated solutions also highly stable; however, extreme caution is needed here.

For the class of nonlinear Hamiltonian oscillator systems to which the Toda lattice belongs, Siegel<sup>8)</sup> has shown that non-integrability is overwhelmingly the general case. Moreover, Saito<sup>9)</sup> and coworkers<sup>10)</sup> have presented computer evi-

dence supporting highly non-integrable behavior for the Toda lattice. If indeed the Toda lattice is highly non-integrable, then the associated lattice soliton would exhibit, under the slightest perturbation, a very slow but observable instability and decay due to Arnold diffusion.<sup>11)</sup> Even worse, for sufficiently large system energy the exact soliton trajectories in phase space would likely occur at the center of extremely small regions of Kolmogorov-Arnold-Moser (KAM) stability<sup>12)</sup> surrounded by an otherwise ergodic sea covering the remaining allowed phase space. Here a small perturbation of the soliton would involve a strong instability yielding a rapid, almost explosive decay into the ergodic sea.

Thus two equally attractive possibilities exist.\*) The Toda lattice is a member of the exception class of integrable oscillator systems, making it a rare jewel in physics—a physically interesting, nonlinear system which can in principle be analytically solved exactly. Alternatively, the Toda lattice is typical of the more general class of non-integrable systems, thereby making it a welcome addition to a small but growing list<sup>9), 12), 18)</sup> of interesting physical models which exhibit stochastic as well as non-stochastic behavior.

In this paper, we attempt to decide between these alternatives by presenting the results of a series of distinct computer experiments. In §2, we discuss a variety of experiments performed for a three-particle Toda lattice, while in §3 we consider a six-particle lattice. In all experiments, periodic boundary conditions are used. Finally, §4 presents our conclusions. Contrary to our original expectations, all our empirical evidence indicates that the Toda lattice is integrable, an unfortunate result from the viewpoint of computer studies. For while a computer can be used to definitively prove non-integrability, it cannot prove integrability, a point we discuss more fully in §§3 and 4. Nonetheless our studies provide such strong support for integrability that we present them in the hope of generating more definitive analytical studies in the future.

## §2. Three-particle Toda lattice

The Hamiltonian for the three-particle Toda lattice with period boundary conditions may be written in the form

$$H = \frac{1}{2}(P_1^2 + P_2^2 + P_3^2) + e^{-(Q_1 - Q_2)} + e^{-(Q_2 - Q_3)} + e^{-(Q_3 - Q_1)} - 3, \quad (1)$$

using the dimensionless variables defined by Toda.<sup>1)</sup> Into Hamiltonian (1), let us now introduce the canonical change of variables

$$Q_i = \sum_{j=1}^3 A_{ij} \zeta_j, \quad P_i = \sum_{j=1}^3 A_{ij} \eta_j, \quad (2)$$

where the matrix  $A$  is given by

---

\*) Actually there is a third possibility, but we defer discussion of it until §4.

$$A = \begin{pmatrix} 6^{-1/2} & 2^{-1/2} & 3^{-1/2} \\ -(2/3)^{1/2} & 0 & 3^{-1/2} \\ 6^{-1/2} & -2^{-1/2} & 3^{-1/2} \end{pmatrix}. \quad (3)$$

We then find

$$H = \frac{1}{2}(\eta_1^2 + \eta_2^2 + \eta_3^2) + e^{-2^{1/2}\zeta_2} + e^{(2^{-1/2}\zeta_2 + (3/2)^{1/2}\zeta_1)} + e^{(2^{-1/2}\zeta_2 - (3/2)^{1/2}\zeta_1)} - 3. \quad (4)$$

Since  $\zeta_3$  is absent from Hamiltonian (4), the conjugate momentum  $\eta_3$  is a constant of the motion corresponding to an uninteresting uniform translation of the lattice. We therefore drop  $\eta_3$  from Hamiltonian (4) and write the equations of motion for the relevant degrees of freedom as

$$\ddot{\zeta}_1 = -(3/2)^{1/2} \{e^{(2^{-1/2}\zeta_2 + (3/2)^{1/2}\zeta_1)} - e^{(2^{-1/2}\zeta_2 - (3/2)^{1/2}\zeta_1)}\}, \quad (5a)$$

$$\ddot{\zeta}_2 = -\{-2^{1/2}e^{-2^{1/2}\zeta_2} + 2^{-1/2}e^{(2^{-1/2}\zeta_2 + (3/2)^{1/2}\zeta_1)} + 2^{-1/2}e^{(2^{-1/2}\zeta_2 - (3/2)^{1/2}\zeta_1)}\}, \quad (5b)$$

where as usual the dot notation is used for time derivatives. In Eq. (5a, b) let  $\zeta_1 = 2\sqrt{2}q_1$ ,  $\zeta_2 = 2\sqrt{2}q_2$  and  $t = \tau/3^{1/2}$ . We then find

$$\ddot{q}_1 = (4\sqrt{3})^{-1} \{-e^{(2q_2 + 2\sqrt{3}q_1)} + e^{(2q_2 - 2\sqrt{3}q_1)}\}, \quad (6a)$$

$$\ddot{q}_2 = (1/6)e^{-4q_2} - (1/12) \{e^{(2q_2 + 2\sqrt{3}q_1)} + e^{(2q_2 - 2\sqrt{3}q_1)}\}, \quad (6b)$$

where we have retained the dot notation for the new  $\tau$  time derivative. With Eq. (6a, b) we may associate the Hamiltonian

$$H = \frac{1}{2}(p_1^2 + p_2^2) + (1/24) \{e^{(2q_2 + 2\sqrt{3}q_1)} + e^{(2q_2 - 2\sqrt{3}q_1)} + e^{-4q_2}\} - (1/8). \quad (7)$$

We now regard Hamiltonian (7) as the basic Hamiltonian for the three-particle Toda lattice with periodic boundary conditions.

Now Whittaker<sup>(14)</sup> asserts that Hamiltonian (7) is integrable provided there exists a second constant of the motion analytic in  $(q_i, p_i)$  which is independent of  $H$  itself. Moreover, several authors<sup>(15)</sup> have demonstrated that one can always develop a formal series expression for this additional constant of the motion. Using the Gustavson procedure,<sup>(15)</sup> we have calculated for Hamiltonian (7) a series expression for this additional constant through eighth order in  $(q_i, p_i)$ .\*) Clearly a computer cannot prove convergence of this formal series even if it were known completely. On the other hand by numerically integrating the equations of motion for a variety of initial conditions, one can determine if the truncated, formal series is a valid constant of the motion to within computer accuracy. In most of our numerical integrations, this series was indeed found to be a constant of the motion exhibiting a time variation only slightly greater than the Hamiltonian itself.

In devising an alternative computer test for integrability, let us suppose that an additional, analytic constant of the motion  $I = I(q_1, p_1, q_2, p_2)$  does exist in ad-

\*) We omit listing this computer generated series for reasons discussed in the last paragraph of § 4.

dition to  $H=H(q_1, p_1, q_2, p_2)$  itself. Then every system trajectory must lie on some smooth two-dimensional integral surface in  $(q_1, p_1, q_2, p_2)$  space. If we now intersect this integral surface with a two-dimensional, plane Poincare surface of section,<sup>10)</sup> we note that each trajectory must intersect the plane surface of section at a set of points lying on a curve. Thus as a test for integrability, we may numerically integrate using a standard fourth-order Range-Kutta method to find a group of trajectories for Hamiltonian (7) at fixed energy and then establish if each trajectory yields a surface of section set of intersection points lying on a curve.

For Hamiltonian (7), we choose to take the  $(q_2, p_2)$  plane as the surface of section. In particular, we choose an initial  $(q_2, p_2)$  point, set  $q_1=0$ , and solve Eq. (7) for  $p_1 \geq 0$ . This gives us an initial  $(q_2, p_2)$  intersection point and an initial condition  $(q_1, p_1, q_2, p_2)$  for integrating a trajectory. The original  $(q_2, p_2)$  point then maps into the next  $(q_2, p_2)$  coordinates of a point on this system trajectory for which  $q_1=0$  and  $p_1 \geq 0$ . Clearly each trajectory yields a unique set of  $(q_2, p_2)$  plane intersection points. In Figs. 1 and 2, we present surfaces of section for Hamiltonian (7) at energies  $E=1$  and  $E=256$ . In each case, all trajectories integrated yield smooth curves in the  $(q_2, p_2)$  plane, indicating that Hamiltonian (7) is integrable. It should be noted that Figs. 1 and 2 survey all the allowed phase space for Hamiltonian (7) since the outermost curve in each figure is the intersection of the energy surface with the  $(q_2, p_2)$  plane;  $(q_2, p_2)$  points lying outside this curve yield unphysical negative values for  $p_1^2$ .

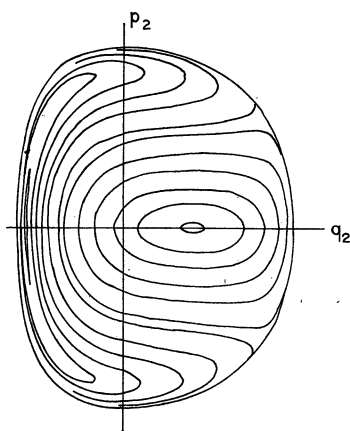


Fig. 1. A surface of section for Hamiltonian (7) at energy  $E=1$ . The scale on both axes is the same. The outermost oval crosses the positive  $q_2$ -axis at  $q_2=1.3$  and the positive  $p_2$ -axis at  $p_2=1.4$ .

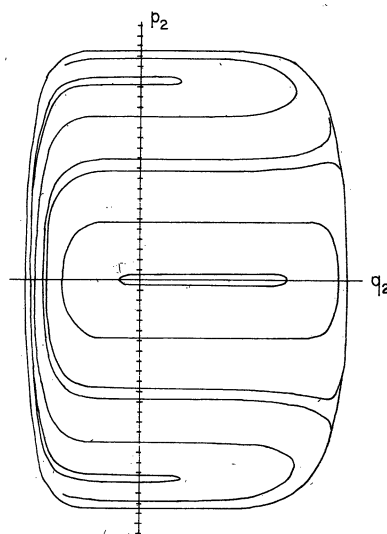


Fig. 2. A surface of section for Hamiltonian (7) at energy  $E=256$ . Here the scale on two axes is not the same. The outermost oval crosses the positive  $q_2$ -axis at  $q_2=4$  and the positive  $p_2$ -axis at  $p_2=22.6$ .

In particular the two unchanging wave form solutions found by Toda<sup>1)</sup> each generate one of the isolated intersection points lying on the  $q_2$ -axis at the center of the two regions of ovals. This connection is discussed more fully in the Appendix.

The full significance of Figs. 1 and 2 is realized if one compares them with the similar figures for the Henon-Heiles Hamiltonian<sup>17)</sup>

$$H = \frac{1}{2}(p_1^2 + p_2^2 + q_1^2 + q_2^2) + q_1^2 q_2 - (1/3)q_2^3 \quad (8)$$

and notes that Hamiltonians (7) and (8) are identical through cubic order in  $q_1$  and  $q_2$ . Indeed it was the possibility of making this connection between Hamiltonians (7) and (8) that led us to introduce periodic boundary conditions in the original Toda lattice Hamiltonian (1). Now Hamiltonian (8) yields smooth curves up to a critical energy of about  $E = (1/10)$ ; then very rapidly as the energy increases to  $E = (1/6)$ , the smooth curves almost completely disappear, indicating non-integrability. Thinking that the somewhat similar Toda Hamiltonian (7) would also be non-integrable, we chose to begin our investigation at  $E = 1$ , only to find smooth curves everywhere. Upping the energy to  $E = 256$ , then to  $E = 1024$  and finally to  $E = 56,000$ <sup>\*)</sup> still yielded smooth curves despite the fact that, at these high energies, the nonlinear terms in Hamiltonian (7) dominate the motion. Thus either Hamiltonian (7) is integrable or else the critical energy is astonishingly large.

As an additional check on integrability, we solved Eq. (7) for  $p_1 \geq 0$  and inserted this expression for  $p_1$  into the formal series for  $I = I(q_1, p_1, q_2, p_2)$  generated by the computer. We thus obtained

$$I = I(q_1, H, q_2, p_2). \quad (9)$$

We then set  $q_1 = 0$  in Eq. (9) and solved for  $p_2$ , obtaining

$$p_2 = p_2(q_2, I, H). \quad (10)$$

Equation (10) yields an independent algebraic expression for the directly integrated curves of Figs. 1 and 2. The algebraic curves computed using Eq. (10) were found to be negligibly different from the directly integrated curves, again indicating the validity of the constant  $I$  and the integrability of Hamiltonian (7).

We now turn to another, more sensitive test for integrability. Let us now, as is permissible,<sup>18)</sup> regard Fig. 1 as a picture of an area-preserving mapping of the  $(q_2, p_2)$  plane onto itself. If Hamiltonian (7) were integrable, then Fig. 1 would everywhere, interior to the bounding curve, be covered with smooth oval curves. On a given oval, sequential mapping iterates rotate around the oval. The average angle of rotation (divided by  $2\pi$ ) is called the rotation number  $\omega$  of the oval, and  $\omega$  varies smoothly as one proceeds out away from either of the fixed points on the  $q_2$ -axis. For an oval with irrational  $\omega$ , iterates of an initial

<sup>\*)</sup>  $E = 56,000$  was the maximum energy we could study and still retain adequate computer accuracy.



Fig. 3. In Fig. 1 if Hamiltonian (7) were non-integrable, then increased computer integration accuracy would reveal a mapping about either fixed point on the  $q_2$ -axis similar to this sketch.

Table I. Typical data for the quantity  $R$  associated with a fixed point. Each line lists, for a given fixed point, the energy, the  $P$  and  $Q$  values ( $\omega=P/Q$ ) for the fixed point, the quantity  $R$ , and the computer error associated with  $R$ . In each case, we see that  $R=0$  within machine error.

Energy	$P$	$Q$	$R$	Error
128	1	5	$1.3 \times 10^{-5}$	$3.8 \times 10^{-5}$
128	2	5	$8.0 \times 10^{-5}$	$5.1 \times 10^{-4}$
128	1	6	$3.9 \times 10^{-5}$	$1.3 \times 10^{-4}$
128	4	11	$2.8 \times 10^{-5}$	$4.9 \times 10^{-5}$
256	1	3	$6.6 \times 10^{-6}$	$2.6 \times 10^{-5}$
256	2	5	$1.0 \times 10^{-5}$	$4.1 \times 10^{-5}$

mapping point densely fill in the oval. However ovals with rational  $\omega=P/Q$ , where  $P$  and  $Q$  are integral, are composed purely of fixed points of  $T^Q$ , where  $T$  denotes a single iteration of the mapping. On the other hand, if Hamiltonian (7) were non-integrable, then sufficient computer accuracy would reveal<sup>18)</sup> a mapping about either of the fixed points on the  $q_2$ -axis similar to that sketched in Fig. 3. This figure shows that many of the ovals (bearing irrational  $\omega$ ) persist. However ovals with rational  $\omega=P/Q$  now longer appear. At their expected position one finds only  $2Q$  fixed points remaining out of the original complete oval of fixed points.

In order to determine whether or not Fig. 1 actually contains the fixed point structure shown in Fig. 3, one must specifically search for such fixed points using the highest computer accuracy available. In particular in Fig. 1, one first determines  $\omega$  as a function of distance from, say, the central fixed point on the positive  $q_2$ -axis. One then searches for fixed points at or near the locations where ovals with rational  $\omega=P/Q$  might occur. For each such fixed point, one computes a quantity  $R$  whose definition<sup>18)</sup> need not concern us here. If  $R=0$  for a fixed point, then that fixed point lies on an "integrable system" oval of fixed points;<sup>19)</sup> if  $R \neq 0$ , then one has located an isolated fixed point of the type shown in Fig. 3.

If an  $R \neq 0$  fixed point were found, one could then seek to locate the associated self-intersecting curves of the type seen in Fig. 3. A computer can be used to locate such curves, if they exist;<sup>20)</sup> and their existence definitively proves non-integrability, though we need not enter into the details here. For Hamiltonian (7) at each of the energies used in Figs. 1 and 2, we located hundreds of fixed points, and for every fixed point located, we found  $R=0$  to within computer accuracy. Typical data is shown in Table I. Moreover for each of a selected

set of fixed points, we recalculated  $R$  several times, sequentially reducing the error to a value of  $10^{-8}$  or less. In these calculations as the error decreased the computed value of  $R$  also decreased, remaining less than or on the order of the error. Since the Henon-Heiles system has easily detectable,  $R \neq 0$  fixed points<sup>18)</sup> at  $E = (1/12)$ , the lack of such fixed points for the Toda lattice at  $E = 256$  is impressive evidence supporting integrability since the value of  $R$  for an  $R \neq 0$  fixed point is expected to increase rapidly with increasing energy.<sup>18)</sup>

Looking forward to the next section, we now consider one last integrability test which is also applicable to systems having more than two degrees of freedom. Let us integrate two trajectories for Hamiltonian (7) which are initially very close together in  $(q_1, p_1, q_2, p_2)$  space. For integrable systems, the distance between these trajectories grows approximately linearly with time; while for non-integrable systems, this distance grows exponentially.<sup>17), 21)</sup> In Fig. 4, we graph the data for a typical trajectory-pair started a distance of about  $10^{-4}$  apart. In order to maintain dimensional homogeneity, we separately plot the spacial distance

$$D_q = [(q_1^{(1)} - q_1^{(2)})^2 + (q_2^{(1)} - q_2^{(2)})^2]^{1/2} \quad (11)$$

and the momentum distance

$$D_p = [(p_1^{(1)} - p_1^{(2)})^2 + (p_2^{(1)} - p_2^{(2)})^2]^{1/2}, \quad (12)$$

where the superscripts in parentheses denote the two members of the trajectory-pair. The straight lines in Fig. 4 represent a least squares fit of the data. The sharp oscillations in Fig. 4 may worry some readers; the essential point is that the average distance here grows approximately linearly by only about one power of ten in the time interval shown. Were this exponential growth, the distance would have grown by many powers of ten in this same time interval.<sup>21)</sup>

Clearly the results of this section do not prove that Hamiltonian (7) is integrable, since a computer cannot investigate every trajectory as would be required for such a proof. Nonetheless the evidence presented lends strong support for integrability.

### § 3. The six-particle Toda lattice

Although the three-particle Toda lattice (which can be reduced to two de-

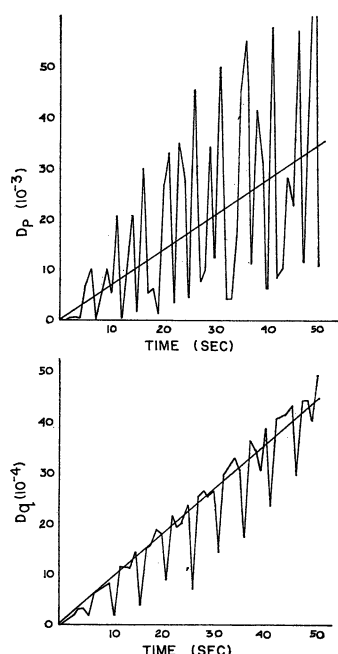


Fig. 4. A typical graph of the distances  $D_q$  and  $D_p$  for Hamiltonian (7). These distances on the average grow linearly with time indicating that Hamiltonian (7) is integrable. Here  $E = 1024$ .

degrees of freedom) appears to be integrable, one could easily argue that it is a special case<sup>22), 28)</sup> and that non-integrability prevails when the number of particles is four or greater. Therefore in this section we discuss a six-particle Toda lattice, again using periodic boundary conditions. The Hamiltonian is

$$H = \frac{1}{2} \sum_{k=1}^6 p_k^2 + \sum_{k=1}^6 e^{-(q_{k+1} - q_k)} - 6, \quad (13)$$

where  $q_7 \equiv q_1$ . As in § 2, we may introduce harmonic normal mode coordinates via

$$q_k = \sum_{j=1}^6 B_{kj} Q_j, \quad p_k = \sum_{j=1}^6 B_{kj} P_j, \quad (14)$$

where the matrix  $B$  is given by

$$B = \begin{pmatrix} 1 & -1 & -1 & 1 & 1 & 1 \\ -1 & -1 & 1 & -1 & 1 & 1 \\ -2 & 2 & -1 & 0 & 0 & 1 \\ -1 & -1 & 1 & 1 & -1 & 1 \\ 1 & -1 & -1 & -1 & -1 & 1 \\ 2 & 2 & 1 & 0 & 0 & 1 \end{pmatrix} \quad (15)$$

and where the columns of  $B$ , thought of as vectors, must be normalized to unity before use in Eq. (14). In normal mode coordinates, Hamiltonian (13) becomes

$$H = \frac{1}{2} \sum_{k=1}^6 (P_k^2 + \omega_k^2 Q_k^2) + \dots, \quad (16)$$

where  $\omega_1 = \omega_5 = 1$ ,  $\omega_2 = \omega_4 = \sqrt{3}$ ,  $\omega_3 = 2$  and  $\omega_6 = 0$ , and the dots indicate cubic and higher order terms in the  $Q_k$ . Here as expected for periodic boundary conditions, the normal mode frequencies are equal in pairs except for the largest and the least. The frequency  $\omega_6 = 0$ , of course, corresponds to the pure translation mode which we neglect in all calculations by initially setting  $Q_6 = P_6 = 0$ .

We first investigate energy sharing among the normal mode degrees of freedom. In particular, we give almost all the energy to a single mode and then plot the energies

$$E_k = (1/2) (P_k^2 + \omega_k^2 Q_k^2) \quad (17)$$

as a function of time. First for total system energy  $E = 1.32$ , we initially set  $E_1 = 1.28$  and  $E_k = 0.01$  for  $2 \leq k \leq 5$ . The results for this case are graphed in Fig. 5. Here one notes an almost periodic behavior and a lack of energy sharing indicating either a non-resonant,<sup>\*)</sup> integrable system or a non-integrable system

<sup>\*)</sup> Actually since certain of the uncoupled, harmonic frequencies are equal in pairs for our system, we would anticipate at least some energy sharing between the mode-pairs having equal frequencies. Indeed an example of this can be seen in Fig. 5 where mode 1 appears to be sharing energy slowly and almost monotonically with mode 5. The mode 5 curve is made up of long followed by short dashes.



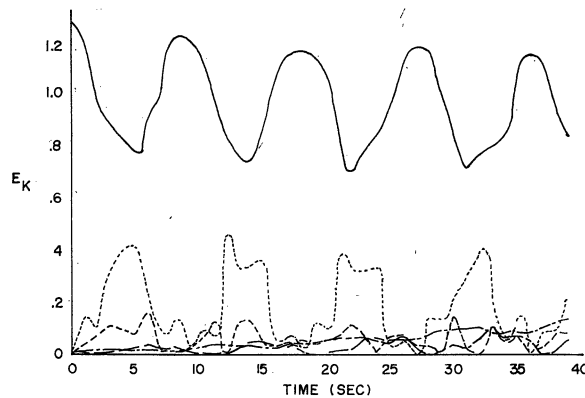


Fig. 5. A graph of the harmonic, normal mode energies  $E_k$  as a function of time. Here the total energy is  $E=1.32$ , while  $E_1=1.28$  and  $E_k=0.01$  for  $2 \leq k \leq 5$  at  $t=0$ . One here notes almost periodic behavior for the system.

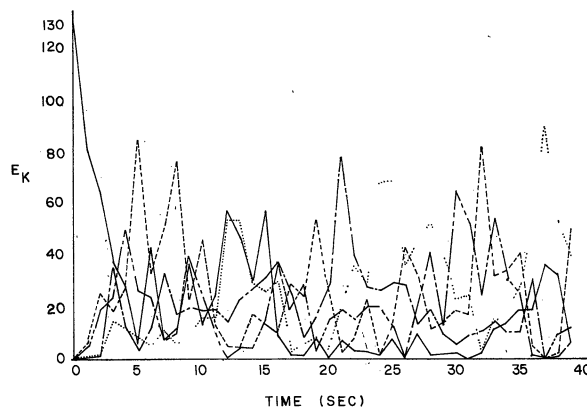


Fig. 6. A graph of the harmonic, normal mode energies  $E_k$  as a function of time. Here the total system energy is  $E=132$ . At  $t=0$ ,  $E_1=128$  and  $E_k=1$  for  $2 \leq k \leq 5$ . Here one notes what appears to be equipartition of energy on the time average.

in its region of KAM stability.<sup>13)</sup> Next for total system energy  $E=132$ , we initially set  $E_1=128$  and  $E_k=1$  for  $2 \leq k \leq 5$ . For this case, we see in Fig. 6 that energy is freely shared among all degrees of freedom and that the almost periodic behavior has disappeared. Apparently one even has equipartition of energy on the time average, but we have not closely investigated this point. Figure 6 indicates that Hamiltonian (13) at this energy is either a resonant, energy sharing, integrable system or else a non-integrable system lying outside its region of KAM stability.

In order to investigate the question of integrability, we integrated a number of initially close trajectory-pairs for both  $E=1.32$  and  $E=132$ . All the trajectory-pairs we investigated gave the same result, namely an almost linear average growth of separation distance with time. Figure 7 shows a graph of  $D_q$  and  $D_p$  for this system using the initial condition of Fig. 6 for one member of the

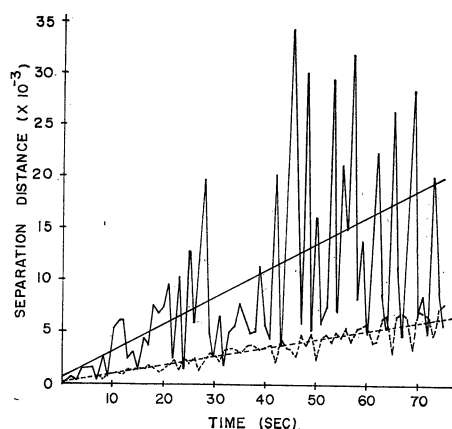


Fig. 7. A graph of  $D_q$  and  $D_p$  versus time for Hamiltonian (13) at energy  $E=132$ . Here the initial conditions for one member of the trajectory-pair were the same as those used in Fig. 6. The average linear growth of separation distance with time indicates that Hamiltonian (13) is integrable even above the transition to energy sharing. Here the  $D_p$  curves are solid while the  $D_q$  curves are dashed.

to non-integrable, ergodic behavior.

Nonetheless, energy sharing and ergodicity are quite distinct properties and nothing in principle requires that they occur together in every case, even for non-integrable systems. More important for the case at hand, nothing in principle precludes a nonlinear, integrable system from making a transition to energy sharing behavior as some system parameter is varied. Indeed once the additional computer evidence, of which our Fig. 7 is typical, is added to the Saito energy sharing results, one concludes that the Toda lattice is precisely this type integrable system. Let us mention in passing that the instability of the soliton in the presence of very large perturbations which was observed by Ooyama and Saito<sup>10</sup> can also be interpreted in terms of an integrable system making a transition to energy sharing behavior. Indeed these authors themselves note that the instability becomes especially pronounced at the energy sharing transition.

In summary, our evidence indicates (but does not prove) that the Toda lattice is integrable. However even if our evidence reflects the true situation, there remains the formidable task of actually calculating the general, analytic solution and studying its properties.

#### § 4. Conclusions

In this paper we have presented computer generated evidence indicating that

trajectory-pair. Our computer study thus indicates that the Toda lattice is integrable even for arbitrary particle number.

Our conclusion is thus at variance with one of the conclusions made by Saito and his coworkers. Saito et al.<sup>9</sup> in § 6d of Ref. 9) consider a fifteen-particle, fixed-end Toda lattice and they obtain graphs of the  $E_k$ -curves for their system looking much like our Figs. 5 and 6. Figure 11 of their paper shows the same type almost periodic behavior seen in our Fig. 5, while their Fig. 9 after a brief induction period shows energy sharing behavior similar to our Fig. 6. Upon this evidence, they conclude that the Toda lattice is non-integrable, a quite reasonable conclusion in view of Siegel's theorem.<sup>8</sup> Indeed most oscillator systems are non-integrable<sup>8</sup> and, in general for them, the transition to energy sharing behavior is congruent with the transition

the Toda lattice is integrable. Although special, analytic, physically interesting solutions for the Toda lattice have been known for some time (see the Appendix), our result indicates that one can, in principle, obtain the general solution in closed, analytic form. Indeed our results make it plausible that an approximate general solution can be obtained using classical perturbation theory,<sup>10)</sup> although the energy sharing property of the Toda lattice may make such calculations prohibitively complicated. Regardless of how obtained, a general solution for the Toda lattice would add greatly to our currently meager physical and mathematical knowledge of nonlinear systems.

In closing, let us counter an objection<sup>5),24)</sup> to this paper which will certainly occur to discerning readers. Let us write Hamiltonian (7) in the convergent power series form

$$H = \frac{1}{2}(p_1^2 + p_2^2 + q_1^2 + q_2^2) + \sum_{j,k,m,n} C_{jkmn} p_1^j p_2^k q_1^m q_2^n, \quad (18)$$

where the sum extends over all cubic and higher powers in the series. Since in Hamiltonian (18) all the  $C_{jkmn}$  are known exactly, integrability for this Hamiltonian is a precisely defined mathematical problem. However the computer does not precisely integrate Hamiltonian (17) because the computer can perform only finite arithmetic. Thus if we modified Hamiltonian (18) by making changes in all the  $C_{jkmn}$  so small that the modified  $C_{jkmn}$  had the same computer representation, then all our computer calculations would be unchanged. In short our computer results indicate integrability for the whole class of Hamiltonians whose  $C_{jkmn}$  differ only very slightly from those of the mathematically precise Hamiltonian (18). But mathematically, this is a nonsense result since Siegel's theorem<sup>8)</sup> states that non-integrable systems are dense in the class of Hamiltonians just described. Physically speaking, however, our computer results have a sensible meaning. Even though most Hamiltonians of the class described are mathematically non-integrable and therefore certainly exhibit the pathology indicated in Fig. 3, the computer calculations reveal that at worst this pathology occupies such a fractionally small phase space region that it may be regarded as physically irrelevant at least up to the extraordinarily large system energies studied. In particular even if the precise Toda Hamiltonian (18) is mathematically non-integrable, one can nonetheless obtain a closed form, analytic solution<sup>5),12),15)</sup> for most of the system trajectories because the computer reveals that this system (as well as the associated class) lies deep within its region of KAM stability<sup>12)</sup> even for extremely large system energy. Thus the strong KAM instability mentioned in § 1, if it occurs at all, does so only for unphysically large energies; equally, the slow Arnold diffusion, if it occurs at all, would require unphysically long time periods to become noticeable. As a consequence at least over a physically interesting energy range, one may conclude with reasonable certainty that most trajectories of the Toda lattice can be described by a closed form, analytic solution.

Here the main body of our original manuscript ended; however we utilize the opportunity given us by a reviewer's request for minor changes in the original manuscript to add the following exciting footnote. Motivated by reading a preprint of this paper, Professor M. Henon sought and found analytic expressions for  $n$  independent constants of the motion for the  $n$ -particle Toda lattice having periodic boundary conditions. Moreover since these  $n$  constants of the motion are in involution, Liouville's Theorem<sup>14)</sup> insures that the Toda lattice with periodic boundary conditions is a completely integrable system. Using Henon's results, it may be shown that the Toda lattice with fixed ends is also a completely integrable system. Henon will soon publish the details of discovery in another place. Here we mention only that Hamiltonian (7) has the exact, independent constant of the motion

$$\begin{aligned} \emptyset(q_1, p_1, q_2, p_2) = & 8p_1(p_1^2 - 3p_2^2) + (p_1 + \sqrt{3}p_2)e^{(2q_2 - 2\sqrt{3}q_1)} \\ & - 2p_1e^{-4q_2} + (p_1 - \sqrt{3}p_2)e^{(2q_2 + 2\sqrt{3}q_1)}. \end{aligned} \quad (19)$$

Since the series expression for the constant of the motion determined by our computer calculation is a complicated function of the  $\emptyset$  given by Eq. (19) and the  $H$  given by Eq. (7), we have elected to present the simpler Eq. (19) rather than the computer result.

### Acknowledgements

The authors are indebted to Professor N. Saito for providing a critical reading of an early draft of this paper and to Professor M. Henon for communicating his discovery to us prior to its publication. Additionally, one of us (JST) wishes to acknowledge helpful discussions with William C. Schieve, John W. Middleton and Herman W. Harrison during the early stages of the work.

### Appendix

We now make more explicit the connection of the results of § 2 with the solitary wave solutions of the exponential lattice found by Toda<sup>1)</sup> and investigated numerically by Saito and others.<sup>9),10)</sup> In physical coordinates the Hamiltonian for the homogeneous, three-particle, exponential lattice with periodic boundary conditions takes the form

$$H = \sum_{n=1}^3 \{ (p_n^2/2m) + (a/b) [e^{-b(r_n-D)} + b(r_n-D) - 1] \}. \quad (A.1)$$

Here  $a$  and  $b$  constants of the lattice,  $p_n$  is the single particle momentum,  $r_n$  is the separation distance between particle  $n$  and  $n-1$  (here  $n=0$  and  $n=3$  refer to the same particle), and  $D$  is the equilibrium (zero-temperature) lattice spacing.

The solitary wave solutions<sup>1)</sup> for the Toda lattice with move without change of wave form may be written down in the closed form

$$e^{-b(\tau_n - D)} = 1 + [m(2K\nu)^2/ab] \{dn^2[2K(yt \mp (n/\lambda))] - (E/K)\}, \quad (\text{A} \cdot 2)$$

where the frequency  $\nu$  of the wave is given by

$$2K\nu = (ab/m)^{1/2} \{[sn(2K/\lambda)]^{-2} - 1 + (E/K)\}^{-1/2}. \quad (\text{A} \cdot 3)$$

In these equations  $K$  and  $E$  are the complete elliptic integrals of the first and second kind, respectively, parameterized by the modulus  $k$ , a measure of the energy of the wave (and therefore of the lattice);  $dn$  and  $sn$  are the standard Jacobian elliptic functions again parameterized by modulus  $k$ . The  $dn$  function is periodic with period  $2K$ , so that  $\lambda$  in Eq. (A·2) is the wavelength of the solitary wave expressed in number of particles, here  $\lambda=3$ . The minus (plus) sign in the argument of  $dn^2$  corresponds to a wave moving in the direction of increasing (decreasing)  $n$ . In the surface of section analysis of § 2 (Figs. 1, 2), the isolated fixed point on the positive  $q_2$ -axis corresponds to the forward (minus sign) running solitary wave, while the one on the negative  $q_2$ -axis is the backward running wave. In particular, one immediately sees from Figs. 1 and 2 that these solitary waves are quite stable in the sense that a trajectory initially near a solitary wave trajectory remains near it for all time.

#### References

- 1) M. Toda, Prog. Theor. Phys. Suppl. No. 45 (1970), 174; J. Phys. Soc. Japan **22** (1967), 431; **23** (1968), 501.
- 2) See F. D. Tappert and C. N. Judice, Phys. Rev. Letters **29** (1972), 130, and F. D. Tappert and N. J. Zabusky, Phys. Rev. Letters **27** (1971), 1774, and the references listed therein.
- 3) See the review article by N. J. Zabusky, Computer Phys. Comm. **5** (1973), No. 1, for discussion and further references.
- 4) V. E. Zakharov and L. D. Faddeev, Funct. Anal. and Appl. **5** (1971), 280.
- 5) J. Moser, Mem. Am. Math. Soc. (1968), No. 81, 1.
- 6) H. Goldstein, *Classical Mechanics* (Addison-Wesley Pub. Co., Inc., Cambridge, Mass., 1951), Ch. 9.
- 7) M. Toda and M. Wadati, J. Phys. Soc. Japan **34** (1973), 18.
- 8) C. L. Siegel, Ann. Math. **42** (1941), 806; Math. Ann. **128** (1954), 144. Also consult Ref. 5) above.
- 9) N. Saito, N. Ooyama, Y. Aizawa and H. Hirooka, Prog. Theor. Phys. Suppl. No. 45 (1970), 209.
- 10) N. Ooyama and N. Saito, Prog. Theor. Phys. Suppl. No. 45 (1970), 201.
- 11) V. I. Arnold, Soviet Math. **156** (1964), 581.
- 12) G. H. Walker and J. Ford, Phys. Rev. **188** (1969), 416.
- 13) J. Ford, Adv. Chem. Phys. **24** (1973), 155.
- 14) E. T. Whittaker, *Analytical Dynamics* (Cambridge University Press, New York, 1965), p. 323.
- 15) G. D. Birkhoff, *Dynamical Systems* (Am. Math. Soc., Prov., R. I., 1966), p. 82.  
G. Contopoulos, Astrophys. J. **138** (1963), 1287.  
F. G. Gustavson, Astron. J. **71** (1966), 670.
- 16) V. I. Arnold and A. Avez, *Ergodic Problems of Classical Mechanics* (Benjamin, New York, 1966), Appendix 31.
- 17) M. Henon and C. Heiles, Astron. J. **69** (1964), 73.
- 18) G. H. Lunsford and J. Ford, J. Math. Phys. **13** (1972), 700.

- 19) J. M. Greene, *J. Math. Phys.* **9** (1968), 760.
- 20) See, for example, J. H. Bartlett and C. A. Wagner, *Celestial Mech.* **2** (1970), 228.
- 21) J. Ford and G. H. Lunsford, *Phys. Rev.* **A1** (1970), 59.
- 22) L. Galgani and A. Scotti, *Phys. Rev. Letters* **28** (1972), 1173. Footnote 23 of this article reports results similar to our Figs. 1 and 2 for a two-particle, Lennard-Jones lattice with fixed-end boundaries. The same type results have been reported in the preprint literature for a two-particle Toda lattice with fixed-end boundary conditions by Professor N. Saito's group.
- 23) P. Bocchieri, A. Scotti, B. Bearzi and A. Loinger, *Phys. Rev.* **A2** (1970), 2013. See the discussion on p. 2018 of this paper.
- 24) L. Galgani and A. Scotti, *Rivista Nuovo Cim.* **2** (1972), 189. See the discussion on p. 198 of this paper.